Interaction of Water with Self-Assembled Monolayers: Neutron Reflectivity Measurements of the Water Density in the Interface Region

D. Schwendel,[†] T. Hayashi,[†] R. Dahint,[†] A. Pertsin,[†] M. Grunze,*[,†] R. Steitz,[‡] and F. Schreiber[§,||]

Angewandte Physikalische Chemie, Universität Heidelberg, Im Neuenheimer Feld 253, D-69120 Heidelberg, Germany, Berlin Neutron Scattering Center, Hahn-Meitner-Institut, Glienicker Strasse 100, D-14109 Berlin, Germany, Stranski-Laboratorium für Physikalische und Theoretische Chemie, Technische Universität Berlin, D-10623 Berlin, Germany, Institut für Theoretische und Angewandte Physik, Universität Stuttgart, D-70550 Stuttgart, Germany, and Max-Planck-Institut für Metallforschung, Heisenberg Strasse 1, D-70569 Stuttgart, Germany

Received October 18, 2002. In Final Form: December 19, 2002

We applied neutron reflectivity measurements to hydrophilic and hydrophobic self-assembled monolayers (SAMs) to probe water density at these interfaces. The measurements were motivated by a previous theoretical study which reported a reduced water density at a hydrophobic surface (Lum, K.; Chandler, D.; Weeks, J. D. *J. Phys. Chem. B* **1999**, *103*, 4570) and by our own computer simulations on the hydration force and water density between two methoxy tri(ethylene glycol) terminated undecylthiolate SAMs adsorbed on gold substrates used to study protein adsorption. These simulations predicted that the surfaces are slightly hydrophobic and are characterized by a reduced water density at the interface (Pertsin, A. J.; Hayashi, T.; Grunze, M. *J. Phys. Chem. B* **2002**, *106*, 12274). In disagreement with the marginal reduction in water density derived in the simulations, the neutron reflectivity measurements reported here indicate an unexpectedly extended (∼4 nm) water layer at the SAM surface with a noticeably reduced density (85−90% of the density of bulk water). The reproducibility of the experimental results with the methoxy tri(ethylene glycol) terminated undecylthiolate SAMs was confirmed with four different samples and by one measurement using a contrast-matched D_2O/H_2O water mixture. We also used neutron reflectivity measurements to study the water density at the water/SAM interface of hydroxy hexa(ethylene glycol) and hydroxy tri(ethylene glycol) terminated undecylthiolate SAMs. Except for one of the hydroxy hexa(ethylene glycol) samples studied, the results are consistent with the presence of bulk water in direct contact with the interface. We also discuss possible artifacts and problems in the analysis. Our results on nonfunctionalized hydrophobic octadecanethiolate and hydrophilic hydroxy-terminated undecylthiolate SAMs give physically unreasonable and nonconclusive models for the water interface on these surfaces, respectively. The best fit of the data for the hydrophobic surface gives an unreasonably low water density, possibly due to the presence of air inclusions in the film and/or adsorbed air "nanobubbles". The results obtained on the hydrophilic hydroxy-terminated surface can be fitted equally well with a model assuming an interface water density that is higher or lower than that of bulk water, demonstrating the ambiguities associated with describing the organic/liquid interface with a box model for the *Q* range accessible in our experiment.

Introduction

One of the pertaining issues in the discussion of the interaction of water with surfaces is the property of water in direct contact with solids. Water molecules adsorbed on a surface are expected to have a preferential orientation caused by the directional nature of the water/substrate bond, which will affect the ability of these water molecules to be integrated into the hydrogen bonding network of surrounding water molecules. This difference in the ability to optimize hydrogen bonding between the water molecules at the solid/liquid interface and the adjacent bulk liquid will affect the structure of interfacial water and hence its static and dynamic properties, as reflected in its density and viscosity. These considerations give rise to the expectation that water in contact with a solid has a different structure and density than bulk water and that in the extreme it may be "icelike" if the density is reduced. A "Biography of Water" discussing the special properties of water and the questions relating to its interfacial properties was presented by P. Ball.[3]

A direct measurement of the structure and density of water at a solid/liquid interface is, to say the least, not straightforward. Experimental results giving indirect information on interfacial water properties were reviewed by Israelachvili[4,5] and Vogler.[6] Direct spectroscopic results proving a preferential orientation of water molecules at solid surfaces,[7,8] the pH dependence of the orientation,[9] and changes in water orientation upon polyelectrolyte or

* Corresponding author.
[†] Universität Heidelberg.
[‡] Hahn-Meitner-Institut and Technische Universität Berlin.
[§] Universität Stuttgart and Max-Planck-Institut für Metallforschung.
[||] Present address: Physical and Theoretical Chemistry Laboratory, South Parks Road, University of Oxford, Oxford OX1 3QZ, U.K.

(1) Lum, K.; Chandler, D.; Weeks, J. D. *J. Phys. Chem. B* **1999**, *103*, 4570.
(2) Pertsin, A. J.; Hayashi, T.; Grunze, M. *J. Phys. Chem. B* **2002**, *106*, 12274.
(3) Ball, P. *H_2O: A biography of water*; Weidenfeld & Nicolson: London, 1999.
(4) Israelachvili, J.; Wennerström, H. *Nature* **1996**, *379*, 219.
(5) Israelachvili, J. *Intermolecular and Surface Forces*; Academic Press: London, 1992.
(6) Vogler, E. A. *Adv. Colloid Interface Sci.* **1998**, *74*, 69.
(7) Du, Q.; Freysz, Y.; Shen, R. *Phys. Rev. Lett.* **1994**, *72*, 238.
(8) Du, Q.; Freysz, Y.; Shen, R. *Science* **1994**, *264*, 826.

10.1021/la026716k CCC: $25.00
Published on Web 02/22/2003

protein adsorption at a solid/water interface[10,11] were recently obtained by vibrational sum frequency generation (SFG). Due to the nature of this nonlinear optical technique, only water molecules adsorbed onto the surface, but not those in adjacent water layers, can be observed. The structural transition of water from adsorbed and preferentially oriented water molecules into the bulk water structure, in particular the range of this transition zone (which we will hereafter call water inter*phase*), remains elusive.

Indirect conclusions on the structure of water confined between two surfaces can be derived from surface force measurements. The dynamical properties of water films confined in narrow slits, in particular its fluidity, have been studied experimentally by surface force balance experiments by Klein et al.[12] and Zhu and Granick.[13] However, the two studies give different results on the properties of the confined water film. A measurement of water density oscillations near a mica/water interface with high-resolution specular X-ray reflectivity was reported by Cheng et al.[14] They interpreted their data on crystallographic well-defined mica surfaces by a model in which a layer of adsorbed, laterally ordered water on the molecularly smooth mica surface is followed by a second nonordered hydration layer, suggesting that the effect of the solid surface on water structure vanishes within a few molecular layers.

The situation regarding interfacial water structure may be different on organic substrates, which are commonly classified according to their macroscopic wetting behavior into hydrophobic or hydrophilic surfaces,[15−17] and where the observed water-mediated forces are often associated with unusual structural properties of the water interphase.[6] According to theoretical work by Lum et al.,[1] a reduced water density in a solid/water interphase is a consequence of the hydrophobic nature of the surface.

The water density at a solid/liquid interface can be determined experimentally by neutron reflectivity (NR) which probes the scattering length density profile along the surface normal and is a proven and powerful method to study adsorption (in particular protein adsorption) at air/solution or solid/solution interfaces.[18] Although several examples of NR measurements on solid/liquid interfaces, including self-assembled monolayers (SAMs), were recently reviewed by Lu and Thomas,[18,19] the possible changes in the density of water in contact with a hydrophobic interface, for example, in the study of octadecyl trichlorosilane (OTS) on silica in contact with water, were not discussed.

In our NR study described here, we are interested in probing the water density at the surface of SAMs adsorbed on a polycrystalline gold substrate. SAMs allow precise control of the solid/water interfacial energy as reflected in the macroscopic contact angle,[15−17] and thiols on Au have been characterized in detail.[20] The system we studied most extensively by neutron reflectivity measurements is methoxy tri(ethylene glycol) terminated undecylthiolate SAMs (EG3-OMe) on polycrystalline gold substrates.[15,21,22] Recently the hydration forces between two adjacent EG3-OMe surfaces were calculated using the grand canonical Monte Carlo (GCMC) technique.[2] The simulations predict, in agreement with SFG experiments,[23] that water penetrates into these films and that they exhibit a typical hydrophobic behavior which is reflected in a slightly reduced interphase water density. We note however that these simulations refer to water confined between two SAMs which are 8−10 nm apart. The situation is therefore not directly comparable to the experiments with a single SAM immersed into bulk water, as described in the discussion section of this paper.

Our paper is organized as follows: First we will describe in detail our experimental procedures and fitting strategies of the reflectivity curves with a box model to extract a density profile of water along the *z* axis away from the substrate surface. Then we present the results we obtained on the density of water near EG3-OMe, hydroxy tri(ethylene glycol) (EG3-OH) and hydroxy hexa(ethylene glycol) terminated undecylthiolate SAMs (EG6-OH) and at nonfunctionalized hydrophobic octadecanethiolate (C18) and hydrophilic hydroxy-terminated undecylthiolate SAM (C11OH) surfaces. We find that the results involve noticeable uncertainty, making it difficult to draw reliable conclusions on interphase water density. The results on more hydrophobic surfaces are most likely obscured by the presence of air inclusions or adsorbed nanoscopic air bubbles, which have been observed previously in the atomic force microscopy (AFM) work of Ishida et al.,[24] Ederth et al.,[25] and Tyrell et al.[26]

Experiments

Chemicals and SAM Preparation. Octadecanethiol (O185-8), 11-mercapto-1-undecanol (44,752-8), and deuterium oxide (15,188-2) from Sigma-Aldrich and absolute ethanol (>99.8 vol %) from Riedel-de Haën were used as received. The synthesis and structure of $HS(CH_2)_{11}(OCH_2CH_2)_3OH$ (EG3-OH), $HS(CH_2)_{11}(OCH_2CH_2)_3OCH_3$ (EG3-OMe), and $HS(CH_2)_{11}(OCH_2CH_2)_6OH$ (EG6-OH) have been described elsewhere.[15,21,27] The SAM preparation is described in refs 21 and 28.

Materials. Onto all-side-polished, single-crystal SiO_2 (0001) substrates (CrysTec, Berlin, Germany), $8.9 \times 3.8 \times 1.3$ cm^3 in size ($10 \times 8 \times 1.3$ cm^3 in the case of EG3-OH and sample II of EG6-OH), a 10−15 nm thick adhesion layer of Cr and then a 20−50 nm thick Au film were deposited by evaporation. The typical root-mean-square (rms) roughness of the metallized substrate was 8.5−11.5 Å as determined by AFM.

Experimental Procedure. All neutron reflectivity measurements discussed in this paper except those with EG3-OH and sample II of EG6-OH were performed at the Neutron Scattering Center at the Hahn-Meitner-Institut in Berlin (BENSC) on the V6 neutron reflectometer.[29] The instrument has a vertical scattering plane and operates with cold source neutrons at a

(9) Scatena, L. F.; Brown, M. G.; Richmond, G. L. *Science* **2001**, *292*, 908.
(10) Kim, J.; Cremer, P. S. *J. Am. Chem. Soc.* **2000**, *122*, 12371.
(11) Kim, J.; Cremer, P. S. *Chem. Phys. Phys. Chem.* **2001**, *8/9*, 543.
(12) Raviv, U.; Laurat, P.; Klein, J. *Nature* **2001**, *413*, 51.
(13) Zhu, Y.; Granick, S. *Phys. Rev. Lett.* **2001**, *87*, 96104.
(14) Cheng, L.; Fenter, P.; Nagy, K. L.; Schlegel, M. L.; Sturchio, N. C. *Phys. Rev. Lett.* **2001**, *85*, 15.
(15) Pale-Grosdemange, C.; Simon, E. S.; Prime, K. L.; Whitesides, G. M. *J. Am. Chem. Soc.* **1991**, *113*, 12.
(16) Prime, K. L.; Whitesides, G. M. *J. Am. Chem. Soc.* **1993**, *115*, 10714.
(17) Laibinis, P. E.; Whitesides, G. M.; Allara, D. L.; Tao, Y.-T.; Parikh, A. N.; Nuzzo, R. G. *J. Am. Chem. Soc.* **1991**, *113*, 7152.
(18) Lu, J. R.; Thomas, R. K. *J. Chem. Soc., Faraday Trans.* **1998**, *94*, 995.
(19) Fragneto, G.; Lu, J. R.; McDermott, D. C.; Thomas, R. K.; Rennie, A. R.; Gallagher, P. D.; Satija, S. K. *Langmuir* **1996**, *12*, 477.
(20) Schreiber, F. *Prog. Surf. Sci.* **2000**, *65*, 151.
(21) Harder, P.; Grunze, M.; Dahint, R.; Whitesides, G. M.; Laibinis, P. E. *J. Phys. Chem. B* **1998**, *102*, 426.
(22) Ostuni, E.; Chapman, R. G.; Holmin, R. E.; Takayama, S.; Whitesides, G. M.; *Langmuir* **2001**, *17*, 5605.
(23) Zolk, M.; Eisert, F.; Pipper, J.; Herrwerth, S.; Eck, W.; Buck, M.; Grunze, M. *Langmuir* **2000**, *16*, 5849.
(24) Ishida, N.; Masanobu, S.; Miyahara, M.; Higashitani, K. *Langmuir* **2000**, *16*, 5681.
(25) Ederth, T.; Liedberg, B. *Langmuir* **2000**, *16*, 2177.
(26) Tyrell, J. W. G.; Attard, P. *Phys. Rev. Lett.* **2001**, *87*, 17.
(27) Prime, K. L.; Whitesides, G. M. *Science* **1991**, *252*, 1164.
(28) Schwendel, D.; Dahint, R.; Herrwerth, S.; Schlörholz, M.; Eck, W.; Grunze, M. *Langmuir* **2001**, *17*, 5717.
(29) Mezei, F.; Goloub, R.; Klose, F.; Toews, H. *Physica B* **1995**, *213/214*, 898.

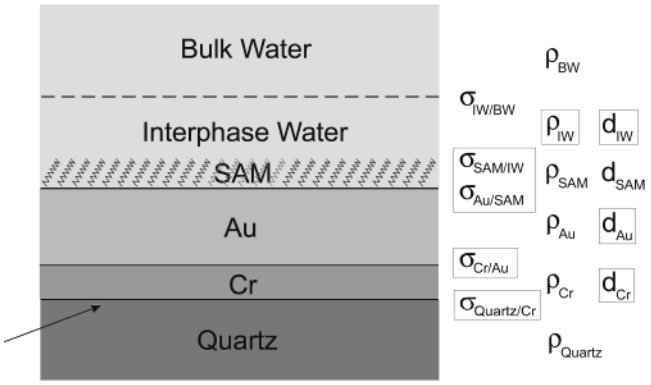

Figure 1. A schematic representation of the multilayer system studied and a list of the associated model parameters. The variable parameters are encircled in a frame. The arrow shows the direction of the incident neutron beam.

wavelength of $\lambda = 4.66$ Å. Instrumental resolution is of the order of 10^{-3} Å^{-1}. Experiments with EG3-OH and sample II of EG6-OH have been performed at the time-of-flight spectrometer D17 at the Institute Laue-Langevin in Grenoble, France. The spectrometer has a horizontal scattering plane and operates in a wavelength range of 2−20 Å with a wavelength resolution $\Delta\lambda$ of 2−15%.

The measurements were made with SAMs both in the dry state and in contact with D_2O and D_2O/H_2O mixtures. In dry-state experiments, the SAM-coated substrates were fixed faceup in an aluminum cell with an O-ring-sealed aluminum lid. The cell was evacuated and flushed with nitrogen several times and finally kept under a small overpressure of nitrogen during the measurement. The wall thickness at the inlet and outlet windows of the aluminum cell was limited to 2 mm each so that the attenuation of the neutron beam was less than 5%.

For the measurements in contact with D_2O, we used a liquid cell as described by McDermott et al.[30]

To verify our results on EG3-OMe, EG3-OH, and EG6-OH in contact with D_2O, we repeated the measurements using a mixture of D_2O and H_2O having a different scattering contrast.[18,19] A mixture of D_2O and distilled water with a ratio of 68:32 vol % or 93:7 vol % has the same scattering length density as quartz or a 15% solution of bovine serum albumin (BSA) in D_2O, respectively. They are denoted as quartz-matched contrast (QMC) and BSA-matched contrast (BSA-MC) in the following. After measurements against pure D_2O, the liquid phase was changed to QMC or BSA-MC and the sample was measured again without further sample adjustment. BSA-MC was used for the EG3-OH SAMs in the context of a research program in which the interaction of BSA with SAM surfaces has been investigated by neutron reflectometry.[31]

Of great concern is the possible damage of the SAMs either during transport or during the measurements. We measured the same EG3-OMe SAM with all instruments used in our neutron reflectivity studies (V6, Hahn-Meitner-Institute, Berlin, and D17, and in addition on the EVA and ADAM reflectometers at the Institute Laue-Langevin, Grenoble, France) within a period of about 4 weeks. The sample was stored in an aluminum container in an inert gas atmosphere (Ar, N_2, or He) and mounted on the liquid cell directly before the measurements. We checked the integrity of the SAM before the first and after the last (fourth) neutron measurement by ellipsometry. Within the error of measurements, we found that the SAM did not change during the 4 weeks of transport and measurements.

Substrate Parameters. To extract the parameters of the system from the measured reflectivity curves, we employed least-squares parametric fitting procedures. The model parameters used to specify the system are the neutron scattering length densities, ρ_i, thicknesses, d_i, and interfacial rms roughnesses, $\sigma_{i/i+1}$, of all the individual layers and interfaces in the system (Figure 1). The scattering length densities of quartz, Cr, Au, and bulk D_2O were fixed at their commonly accepted values.[32] For the QMC and BSA-MC liquid phase, we used a scattering length density of 4.17×10^{-6} and 5.86×10^{-6} Å^{-2}, respectively.

SAM Parameters. The SAM thickness in the dry state was determined by X-ray photoelectron spectroscopy (XPS) and ellipsometry measurements. The values are 20.3 Å for EG3-OH, 29.0 Å for EG6-OH, 20.5 Å for C18, and 13.2 Å for C11OH. For EG3-OMe, the SAM thickness has been measured by four different experimental methods (ellipsometry, XPS, and X-ray and neutron reflectivity) and proved to be in the range from 20 to 23 Å. For the analysis of the experiments, the C18 and C11OH areal density was fixed at 21.65 Å^2 per molecule, corresponding to a perfect monolayer of dodecylthiolate (C12) assembled on a Au(111) surface.[33−36] The oligo(ethylene glycol) (OEG) SAMs, however, have a lower coverage than the C18 SAMs.[21,37] According to the XPS measurements, the average molecular areas are 27 Å^2 (EG3-OH and EG3-OMe) and 28 Å^2 (EG6-OH), respectively.

For the EG3-OMe SAM in contact with D_2O, two independent models of the SAM structure were tested. In one model, the SAM is assumed to be impenetrable to water, so that its thickness in contact with water is the same as in the dry state. In the parameter fitting, the thickness is fixed at the mean value of 21.5 Å, which results in $\rho_{SAM} = 1.110 \times 10^{-7}$ Å^{-2}. The other model is based on recent SFG experiments[23] and computer simulations,[2] which show a substantial conformational disordering of the SAM and penetration of water deep into the EG3-OMe layer. The water and SAM density distribution found in computer simulations[2] for two parallel $S(CH_2)_3-(OCH_2CH_2)_3-OCH_3$ SAMs (EG3-OMe with shorter alkyl chain) whose substrates are $H =$ 80 Å apart is depicted in Figure 2. The density distribution is naturally divided into three distinct layers with substantially different scattering length densities: (I) the alkanethiol layer of the SAM ($z < 4$ Å), (II) the interpenetration layer (4 Å $< z <$ 20 Å), and (III) the water layer adjacent to the SAM (20 Å $< z <$ 40 Å). The averaging of the water density in the two latter layers gave 11.5% and 92.2% bulk water density, respectively. A correction for the difference in the alkane chain length between the simulations ($n = 3$) and experiments ($n = 11$) gives for layer I a thickness of 11.3 Å. The subsequent calculations of neutron reflectivity from the EG3-OMe-terminated SAM showed, however, that the division of the SAM into separate alkanethiol and EG3-OMe sublayers had a negligible effect on the calculated reflectivities because of the limited Q range of the measurements. For this reason, in the parameter fitting the SAM was treated as a single layer with a total thickness of $11.3 + 14 = 25.3$ Å and an average scattering length density of 7.349×10^{-7} Å^{-2}.

For EG3-OH, EG6-OH, C18, and C11OH in contact with water, respective computer simulations are not completed yet. Neither experimental nor simulated data on the water penetration are available. For EG3-OH and EG6-OH, we assumed the same swelling and water penetration as for the EG3-OMe-terminated SAMs.[2] This yielded a SAM thickness of 24.1 Å for EG3-OH and 36.6 Å for EG6-OH. Accordingly, the values of ρ_{SAM} used in our fits were 1.505×10^{-7} Å^{-2} (7.689×10^{-7} Å^{-2}) for EG3-OH, 9.123×10^{-8} Å^{-2} (7.260×10^{-7} Å^{-2}) for EG6-OH, -3.576×10^{-7} Å^{-2} for C18, and -1.484×10^{-7} Å^{-2} for C11OH. The values in brackets refer to the swollen SAM in D_2O. Water penetration and SAM swelling in QMC and BSA-MC result in $\rho_{SAM} = 7.201 \times 10^{-7}$ Å^{-2} (EG3-OH/BSA-MC), 5.119×10^{-7} Å^{-2} (EG3-OMe/QMC), and 4.990×10^{-7} Å^{-2} (EG6-OH/QMC).

Water Models. Two different assumptions for the water density distribution next to the SAM surfaces were tested. In the first case, water is represented by a single semi-infinite box with a density equal to that of bulk water (BW). Alternatively, one or two additional boxes, associated with interphase water layers

(30) McDermott, D. C.; Lu, J. R.; Lee, E. M.; Thomas, R. K. *Langmuir* **1992**, *8*, 1204.
(31) Schwendel, D.; Dahint, R.; Schreiber, F.; Grunze, M. To be published.
(32) Russell, T. P. *Mater. Sci. Rep.* **1990**, *5*, 171.
(33) Camilone, N., III; Chidsey, C. E. D.; Liu, G.-Y.; Putvinski, T. M.; Giacinto, S. *J. Chem. Phys.* **1991**, *94*, 8493.
(34) Dubois, L. H.; Zegarsky, B. R.; Nuzzo, R. G. *J. Chem. Phys.* **1993**, *98*, 678.
(35) Fenter, P.; Eisenberger, P.; Liang, K. S. *Phys. Rev. Lett.* **1993**, *70*, 2447.
(36) Schreiber, F.; Eberhard, A.; Leung, T. Y. B.; Schwartz, P.; Wetterer, S. M.; Lavrich, D. J.; Berman, L.; Fenter, P.; Eisenberger, P.; Scoles, G. *Phys. Rev. B* **1998**, *57*, 12476.
(37) Herrwerth, S. Ph.D. Thesis, Ruprechts-Karls Universität, Heidelberg, 2002.

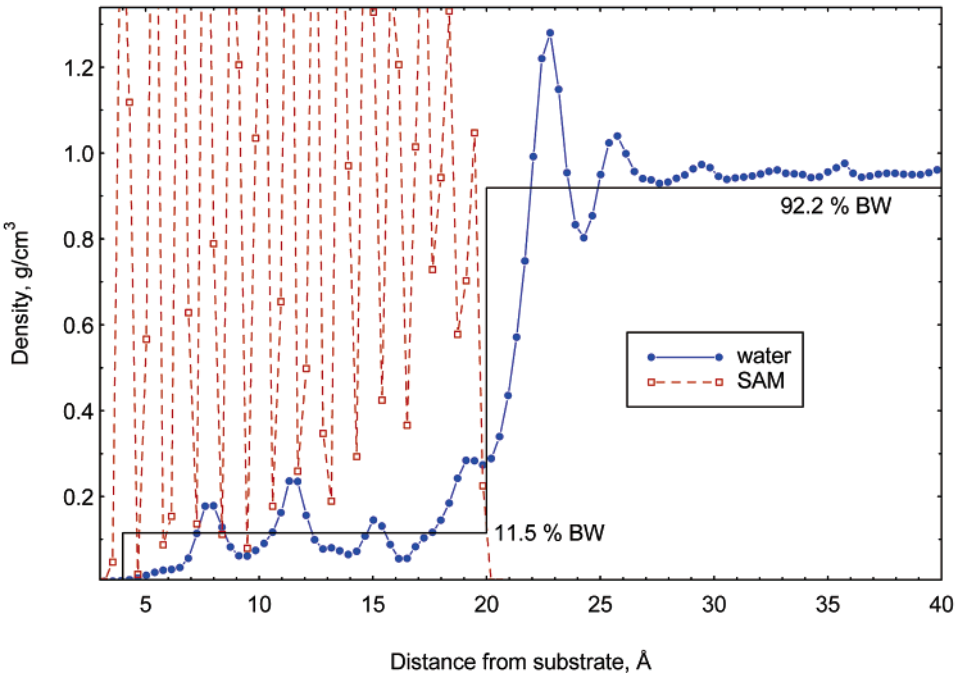

Figure 2. Density profiles in the EG3-OMe SAM−water interfacial region averaged over a SAM area of 36 Au−S(CH)$_3$(OCH$_2$-CH$_2$)$_3$OCH$_3$ thiolate molecules, as obtained in GCMC simulations (ref 2). The blue data points show the density of water molecules as a function of distance from the substrate surface. The red data points depict the SAM density. See details in the text.

(IW), are placed between the SAM and bulk water. The three corresponding models are characterized by the total number n of water boxes and denoted as n-box models in the following. Both the thickness and scattering length density of the individual IW boxes are treated as adjustable parameters, whereas the roughness of each D_2O/D_2O interface (IW_{n-1}/BW and, if existing, IW_1/IW_2) is fixed at zero. While a realistic description may have to include a certain degree of smearing of the density profile at this interface (represented by a finite $\sigma_{IW/BW}$), our assumption reduces the number of fitting parameters and thus the ambiguity of the fitting results. Since our assumption is used consistently throughout the fitting, the results for different films should be comparable and the qualitative conclusions should not be affected.

Fitting Procedure. Due to the so-called "phase problem", there is no general inversion procedure of scattering data. Because the experimental reflectivity (or scattering) pattern is proportional to the square of its complex scattering amplitude, the phase information is in general lost and the corresponding real-space profile cannot be retrieved in an unambiguous manner. The common way of treating the reflectivity problem is to model the interface in real space, subdivide it into a suitable number of slices (boxes) of constant refractive index according to the underlying physical constraints (e.g., the number of layers assembled on the given substrate), and calculate the corresponding reflectivity pattern by applying the dynamical scattering theory. In this respect, mostly the optical matrix method[38] and Parratt's recursion algorithm[32] are applied. The box models are then refined by least-squares fitting procedures to maximize the overlap between the experimental and calculated reflectivity curves and, hence, minimize the merit function χ^2. The model profile that represents the experimental reflectivity curve best in concordance with the physical boundary conditions is accepted as the (most likely) profile of the interface under consideration.

Recently it has been shown both theoretically[39,40] and experimentally[41] that in special cases the phase problem can be overcome by introducing reference layers or, alternatively, by changing the environment. Both strategies are difficult to adapt to our particular problem. The introduction of a magnetic reference layer would change the growth of the Au, and thus the obtained profiles would be difficult to compare with previous data. A systematic change of the scattering length density of the liquid environment is a possibility to reduce the phase problem, but such time intensive measurements may induce changes in the SAM/liquid interphase region and are therefore not further pursued in our studies focusing on the organic/water interface. Replacing the quartz substrate by a silicon substrate is also not favorable because one would treat two individual (and maybe different in their roughness and homogeneity) systems as a single one. This presumption would be hardly justified in our case considering the observed differences in thickness and roughness of the individually prepared systems of the same kind. Therefore, we decided to follow the widespread strategy of least-squares fitting of box models to our reflectivity data.

All the model parameters treated as variables in the fitting routine are shown enclosed in a frame in Figure 1. The variation of two roughness parameters was constrained by the following conditions: $\sigma_{Au/SAM} = \sigma_{SAM/IW1}$ for the two- and three-box models, or $\sigma_{Au/SAM} = \sigma_{SAM/BW}$ for the one-box model; that is, the roughnesses of the upper and lower interfaces of the SAM with the adjacent phases (water and gold) were assumed to be equal. This assumption is justified by the fact that the SAM thickness is small and, to a good accuracy, constant. As a consequence, the SAM conforms to the substrate surface, reproducing its shape and roughness. In Figure 1, $\sigma_{Au/SAM}$ and $\sigma_{SAM/IW1}$ are enclosed in a common frame to emphasize the correspondence between these two parameters. Considering these constraints, the total number of adjustable model parameters is 5, 7, and 9 in the one-, two-, and three-box models, respectively.

The search for the optimum model fit was carried out by minimizing the discrepancy factor χ^2 defined as the sum of weighted squared deviations between the experimental and calculated reflectivities. Two alternative choices for the weighting factors, w, were tried: $w = 1/R^{exp}$ and $w = 1/\Delta R^{exp}$, where ΔR^{exp} is the experimental error in the measured reflectivities R^{exp}. Inasmuch as $\Delta R^{exp} \sim (R^{exp})^{1/2}$, the $1/R$ weighting scheme makes the discrepancy factor more sensitive to the range of higher Q, while the $1/\Delta R$ weighting favors the lower Q range.

In addition, two different strategies were used to check whether the obtained fitting parameters are suitable to correctly describe the studied multilayer system. First, for the liquid-phase

(38) Leckner, J. *Theory of Reflection*; Martinus Nijho: Dordrecht, 1987.
(39) Lipperheide, R.; Weber, M.; Leeb, H. *Physica B* **2000**, *283*, 242.
(40) Zimmermann, K.-M.; Tolan, M.; Weber, R.; Stettner, J. D.; Doerr, A. K.; Press, W. *Phys. Rev. B* **2000**, *62*, 10377.
(41) Majkrzak, C. F.; Berk, N. F.; Krueger, S.; Dura, J. A.; Tarek, M.; Tobias, D.; Silin, V.; Meuse, C. W.; Woodward, J.; Plant, A. L. *Biophys. J.* **2000**, *79*, 3330.

Table 1. Preferred Two-Box Models for Three Investigated OEG SAMs: EG3-OMe against D_2O (a) and QMC (b), EG6-OH against D_2O (c) and QMC (d), and EG3-OH against D_2O (e) and BSA-MC (f)[a]

	EG3-OMe SAM		EG6-OH SAM		EG3-OH SAM	
contrast	(a) D_2O	(b) QMC	(c) D_2O	(d) QMC	(e) D_2O	(f) BSA-MC
no. of samples	4	1	2	1	1	1
no. of boxes	2	2	2	2	2	2
d_{IW} [Å]	41.3 ± 9.3	49	45.5 ± 10.5	28	8	33
	(41.8 ± 8.8)	(48)	47.5 ± 6.5)	(31)	(3)	(32)
ρ_{IW} [$\times 10^{-6}$ Å^{-2}]	5.52 ± 0.29	3.56	5.80 ± 0.13	3.98	6.57	5.89
	(5.55 ± 0.17)	(3.61)	(5.79 ± 0.32)	(4.09)	(6.45)	(5.89)
$\rho_{IW}/\rho_{BW} \times 100$ [%]	86.4 ± 4.4	85.4	91.2 ± 2.3	95.3	103	101
	(86.9 ± 2.6)	(86.6)	(90.8 ± 5.1)	(98.1)	(101)	(101)
$(\chi_1^2/\chi_2^2)_{1/R}^{1/2}$	1.54−2.78	3.15	1.21−2.63	1.21	1.76	1.00
	(1.81−3.43)	(2.32)	(1.21−1.66)	(1.01)	(1.89)	(1.00)
$(\chi_1^2/\chi_2^2)_{1/\Delta R}^{1/2}$	1.33−1.83	6.07	0.97−1.54	0.99	1.83	1.40
	(1.33−1.94)	(4.96)	(1.11−1.45)	(1.03)	(1.94)	(1.00)

[a] The number of samples used to derive the results is given in the third line. All values in brackets refer to the swollen SAM.

measurements the total metal layer thickness d_{Cr+Au} was also estimated from the width of the Kiessig fringes in the regime $Q > 0.02$ Å^{-1} from the linear regression $Q_n = (2\pi/d)n$ where Q_n denotes the maximum position of Kiessig fringe n observed in the reflectivity profile. Taking into account an experimental step width of $\Delta\theta = 0.02°$, d_{Cr+Au} can be determined with a precision of at least ±15 Å. Second, for some of the substrates, dry-state neutron reflectivity measurements against a nitrogen atmosphere were performed to independently determine the metal thickness and roughness. In either case, fitting results for the liquid-phase measurements were accepted only if the calculated parameters for the metal thickness did not differ by more than 15 Å from the independently determined values.

Note that the metal thickness and roughness determined in the dry-state experiments were not used as fixed parameters in the fitting routines for the liquid-phase measurements. This is based on the consideration that the data are uncertain to some extent and that small deviations from these values already have a major impact on the quality of the fit. Moreover, such a procedure would completely fix all parameters in the case of the one-box model, which appears as a too severe restriction considering the inherent uncertainties in the metal layer thicknesses.

All of the calculations were made using the Paratt32 software,[42] which implements Parratt's recurrent formalism for reflectivity,[43] with roughness included as suggested by Névot and Croce.[44]

Results

All detailed fitting results, including substrate parameters (such as metal thickness and roughness) and SAM roughness, are documented in the Supporting Information of this paper.

EG3-OMe. The fitting results for EG3-OMe in contact with D_2O are summarized in Table 1a. These data present the averaged values for the interphase water layer as represented by the two-box model, where the values in brackets refer to the fit assuming a water-swollen SAM.

Aside from the optimum value for the scattering length density ρ_{IW1}, Table 1a gives also the quantity $\rho_{IW1}/\rho_{BW} \times 100$, which represents the interphase water density expressed as a percentage of the bulk density. The ratios $(\chi_1^2/\chi_2^2)_{1/R}^{1/2}$ in Table 1a characterize the improvement obtained when the interphase water box is added to the one-box model (the subscripts 1 and 2 refer to the one- and two-box models, respectively). The higher the $(\chi_1^2/\chi_2^2)_{1/R}^{1/2}$, the more significant the improvement. For comparison, Table 1a also presents the improvement criteria $(\chi_1^2/\chi_2^2)_{1/\Delta R}^{1/2}$ calculated for the same model parameters but using the $1/\Delta R$ weighting scheme. All numbers in brackets refer to the assumption of a swollen SAM with 11.5% of bulk water penetration as described above.

The smallest improvement $(\chi_1^2/\chi_2^2)_{1/R}^{1/2}$ in the quality of fit observed for an individual sample on going from the one-box model to the two-box model is 1.54 (1.81). To estimate the statistical significance of this improvement, we resorted to the Hamilton test.[45] The hypothesis to be tested is that the one-box model, which involves no interphase water, correctly describes the sample structure. On the basis of the number of observations (reflected intensities) and variable parameters, we find from the Hamilton tables[45] that the hypothesis can be rejected at a significance level of 99.5% and higher, that is, the $(\chi_1^2/\chi_2^2)_{1/R}^{1/2}$ criterion strongly favors the two-box model.

The interphase water layer parameters determined in independent measurements using four different samples are in fairly good agreement, the mean values being 41.3 (41.8) Å for thickness and 86.4 (86.9)% for density (the values in brackets refer to the swollen SAM). Since the assumption of both a swollen and a nonswollen SAM results in nearly the same water interphase, it may be concluded that the shape of the reflectivity profile is predominantly determined by the existence of a density-reduced interphase water layer and not by the internal SAM structure.

Figure 3a compares the experimental neutron reflectivity of one of the four samples with the relevant reflectivity curves of the one- and two-box models calculated for a swollen SAM. Noticeable deviations of the one-box model predictions (red line) from the experimental results around $Q < 0.02$ Å^{-1}, in the range 0.05 Å^{-1} < Q < 0.08 Å^{-1}, and particularly at $Q > 0.1$ Å^{-1} are apparent. For the two-box model (green line), a much better correlation is obtained. Figure 3b shows the real-space profile for both models, as obtained between the Au layer and the bulk water phase. While in the case of the one-box model the increase from ρ_{SAM} to ρ_{BW} occurs in one step (red line), the interphase water layer is represented by an additional box at about 340−380 Å (green line) away from the quartz substrate. It can also be observed in Figure 3b that the total metal layer thickness, as calculated by the use of both models, amounts to about 310 Å with a difference of less than 15 Å.

Aside from the above-described fitting strategy summarized in Table 1a, some alternative approaches were tried to see whether the conclusion regarding the preference of the two-box model is independent of the fitting

(42) Braun, C. Ph.D. Thesis, Hahn-Meitner-Institut, Berlin, 1999.
(43) Parratt, L. G. *Phys. Rev.* **1954**, *95*, 359.
(44) Névot, L.; Croce, P. *Rev. Phys. Appl.* **1980**, *15*, 761.
(45) Hamilton, W. C. *Acta Crystallogr.* **1965**, *18*, 502.

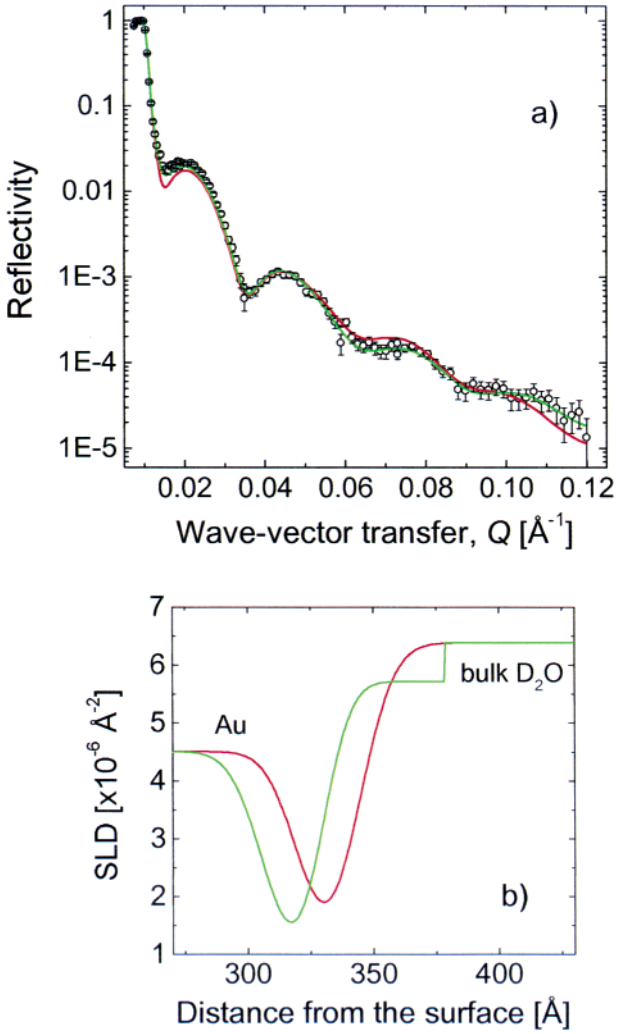

Figure 3. Comparison of the experimental data (circles) and calculated neutron reflectivity (a) and scattering length density profiles (b) for one of the EG3-OMe samples against D_2O. Red line: the model assuming the SAM is in direct contact with the bulk water phase (one-box model). Green line: the model assuming an IW layer of reduced density is between the SAM and the bulk water phase (two-box model).

details and assumptions. When, for example, $\sigma_{SAM/BW}$ was treated as an additional independent parameter in the one-box model, no significant improvement was obtained, that is, the associated change in $(\chi_1^2/\chi_2^2)^{1/2}$ was very small.

For one sample, we also tried to fit the data by fixing the substrate parameters at the values determined independently from a dry-state experiment against a nitrogen atmosphere. The resulting $(\chi_1^2/\chi_2^2)^{1/2}$ criteria were found to be 2.0 and 1.18 for the $1/R$ and $1/\Delta R$ weightings, respectively, which also favors the two-box model. Finally, for all the four samples other fits were tried to achieve satisfactory correlation using (i) a one-box model with free variation of $\sigma_{SAM/BW}$ and $\sigma_{Au/SAM}$ and (ii) a kind of constrained fitting in which $\sigma_{Au/SAM}$ was fixed at 10 Å, as found by AFM for the rms roughness of the bare metallized substrate, while $\sigma_{quartz/Cr}$, $\sigma_{Cr/Au}$, d_{Cr}, and d_{Au} were kept constant at the respective means of the one- and two-box model values determined in unconstrained fits for each individual sample. In all cases, the improvement criteria $(\chi_1^2/\chi_2^2)^{1/2}$ strongly suggested the existence of an extended interphase water layer with a substantially reduced density.

To confirm the above-mentioned results, one experiment has been performed using a quartz-matched contrast.[19,18] These results are summarized in Table 1b. The best fit is obtained with a two-box model similar to the one used for the data set against pure D_2O. The thickness of the interphase water is confirmed to be 49 (48) Å with a density of 85.4 (86.6)% bulk water. The neutron reflectivity data of EG3-OMe against QMC including the fits assuming a "dry" SAM are presented in Figure 4. Both box models do not describe the $Q < 0.016$ Å^{-1} range. Since total external reflection cannot be measured under QMC conditions, it is impossible to normalize these data to an absolute reflectivity. Thus, the normalization parameters for the fits were taken from the experiment against pure D_2O which was performed immediately before. As the sample position might have slightly shifted during the change of the liquid phase to QMC, the deviation in the low Q range is not unexpected. Furthermore, due to lower counting rates especially in the low Q range the experimental error is higher compared to the measurements against D_2O. Thus, the values for the fits given in Table 1b refer only to the $Q \geq 0.016$ Å^{-1} range. The small difference in d_{Cr+Au} is most likely also related to small changes in the sample position and reflects the experimental problems associated with carrying out a series of measurements on one sample outside the range of total reflectivity.

As described in the experimental section, the quality of the SAM is a possible source of error in our data analysis process since we have to assume a certain thickness and water content of the SAM. The presence of defects should obviously enhance the penetration of water into the SAM, so that its scattering length density should also increase. To assess the effect of the SAM imperfections on its water penetrability, we simulated the behavior of water near a SAM in which every sixth lattice site was assumed vacant (the respective monolayer coverage being about 83%). The resulting average density of penetrated water proved to be 20% of the bulk water density. The use of this value in the box-model fitting of the neutron reflectivity data for the sample measured against D_2O and QMC worsened the agreement between the experimental and model reflectivities, particularly in the range 0.016 Å^{-1} < Q < 0.035 Å^{-1}. In addition, the fitting resulted in a physically unrealistic value for the thickness of the metal layer. Similar results were obtained when the density of penetrated water was assumed to be 30% of the bulk water density.

EG6-OH and EG3-OH. To determine whether the observed reduction in the interfacial water density reflects the intrinsic hydrophobicity of the oligo(ethylene glycol) SAM surface, neutron reflectivity studies were also performed on two samples of EG6-OH and one of EG3-OH. Note that SAMs of EG3-OMe, EG3-OH, and EG6-OH on Au are protein resistant[15,16] and exhibit a helical or amorphous conformation of the EG moieties in the dry state[46,37] but differ significantly in their contact angles ($\theta_{adv} = 63 \pm 2°$ for EG3-OMe, $\theta_{adv} = 32-36°$ for EG3-OH, and $\theta_{adv} = 30-35°$ for EG6-OH; θ_{adv}, advancing water contact angle).[37,46] Table 1c presents the averaged fitting results for EG6-OH in contact with D_2O. Values in brackets refer to the results obtained for the swollen SAM. Besides the measurement at the V6 spectrometer (sample I), a second sample of EG6-OH (sample II) was measured against D_2O and QMC at a second beam line (D17, Grenoble). For the liquid-phase measurement of sample I, a significant improvement as compared to the one-box model is again achieved by using a two-box model for the

(46) Harder, P. Ph.D. Thesis, Ruprecht-Karls Universität, Heidelberg, 1999.

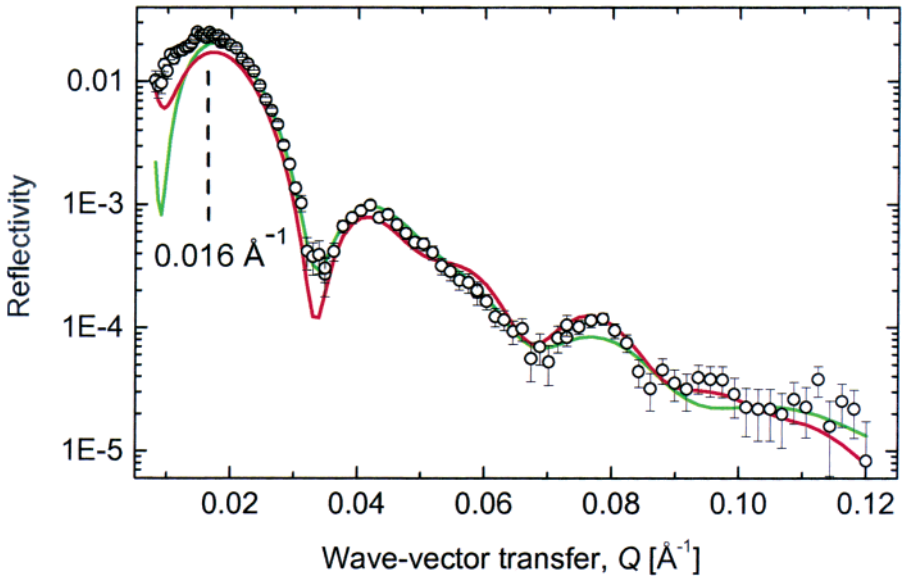

Figure 4. Comparison of the experimental data (circles) and calculated neutron reflectivity profiles for EG3-OMe against QMC. Red line: the model assuming the SAM is in direct contact with the bulk water phase (one-box model). Green line: the model assuming an IW layer of reduced density is between the SAM and the bulk water phase (two-box model).

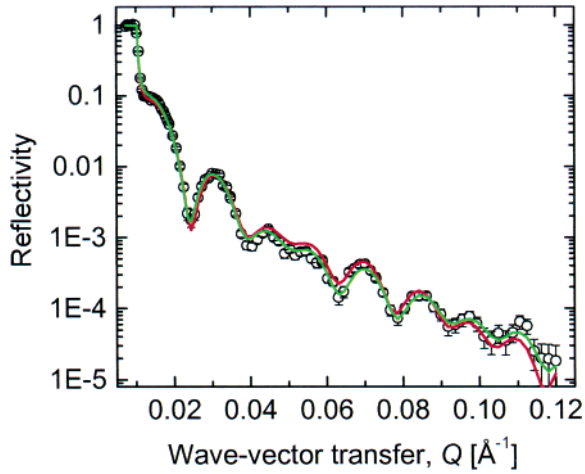

Figure 5. Comparison of the experimental data (circles) and calculated neutron reflectivity profiles for EG6-OH against D_2O. Red line: the model assuming the SAM is in direct contact with the bulk water phase (one-box model). Green line: the model assuming an IW layer of reduced density is between the SAM and the bulk water phase (two-box model).

fit as indicated by the $(\chi_1^2/\chi_2^2)^{1/2}$ values of 2.63 (1.66) and 1.54 (1.45) for the $1/R$ and $1/\Delta R$ weighting schemes. The optimum fit yields an interfacial water layer with a thickness of 56 (54) Å and a reduced density of 88.9 (85.7)% compared to bulk D_2O, which is comparable to the results obtained for EG3-OMe. For sample II, the optimum fits for the $1/R$ and the $1/\Delta R$ weighting schemes indicate a more bulk-water-like interfacial water layer with a thickness of 35 (41) Å in D_2O and 28 (31) Å in contact with QMC (see Table 1d) and a density of 93.4 (95.9)% and 95.3 (98.1)%, respectively.

The neutron reflectivity profile obtained for sample I is presented in Figure 5. Here again, attempts to interpret the experimental data by allowing a free variation of $\sigma_{SAM/BW}$ did not lead to satisfactory agreement.

As described above for EG3-OMe, we tested the quality of the fit as a function of water penetration into the film. Note that in the case of EG6-OH no theoretical or experimental values for the swelling behavior are presently available. For sample I of EG6-OH against D_2O, the best one-box model is achieved for a SAM water density of 30%. Although an acceptable correlation can be achieved, it is improved with the addition of an interphase water layer with a thickness of 41 Å and a density of 92.5%. The corresponding ratio $(\chi_1^2/\chi_2^2)^{1/2}$ yields a factor of 1.80 for $1/R$ and 1.40 for the $1/\Delta R$ weighting scheme. Thus, for all assumed water densities in the swollen SAM (0, 10, 20, 30, and 40%), the two-box model shows better correlation with the reflectivity data than the corresponding one-box model. The exception is sample II, for which a satisfying correlation is achieved using a one-box model and a penetrated water density of 30%. The addition of an interphase water layer does not improve the $(\chi_1^2/\chi_2^2)^{1/2}$ ratio. In contact with QMC, sample II is also best fitted with a one-box model and a penetrated water density of 30%. In summary, the box-model analysis of the reflectivity data for the hydrophilic EG6-OH SAM gives different interphase water densities for different samples, which reflects either the uncertainties involved in fitting the data or the problems associated with a reproducible preparation of the large-area films. Taken together, the results favor a model in which the water density at these hydrophilic hydroxy-terminated surfaces is close to that of bulk water.

In contact angle measurements, EG3-OH shows the same hydrophilicity as EG6-OH. The best fits to the neutron reflectivity measurements of EG3-OH in contact with D_2O and BSA-matched contrast are shown in Table 1e,f. Although the fitting results in case of D_2O show clear improvement for the two-box model, this model assumes a very thin interphase water layer of slightly enhanced density. The two-box model fit for the measurement against D_2O results in a thickness of 8 (3) Å and a density of 103 (101)%. The values for the swollen SAM are given in brackets. For the measurement against BSA-matched contrast, the fits yield an interface water layer of 33 (32) Å with a density of 101 (101)%. In other words, the water interphase at the EG3-OH SAMs cannot be distinguished from bulk water within the uncertainties of our measurements.

C18 and C11OH. We measured a hydrophobic C18 ($\theta_{adv} = 115 \pm 2°$) and two hydrophilic C11OH ($\theta_{adv} = 29 \pm 2°$) alkanethiolate SAM samples on Au. The packing density in these films is about 20% higher than in the

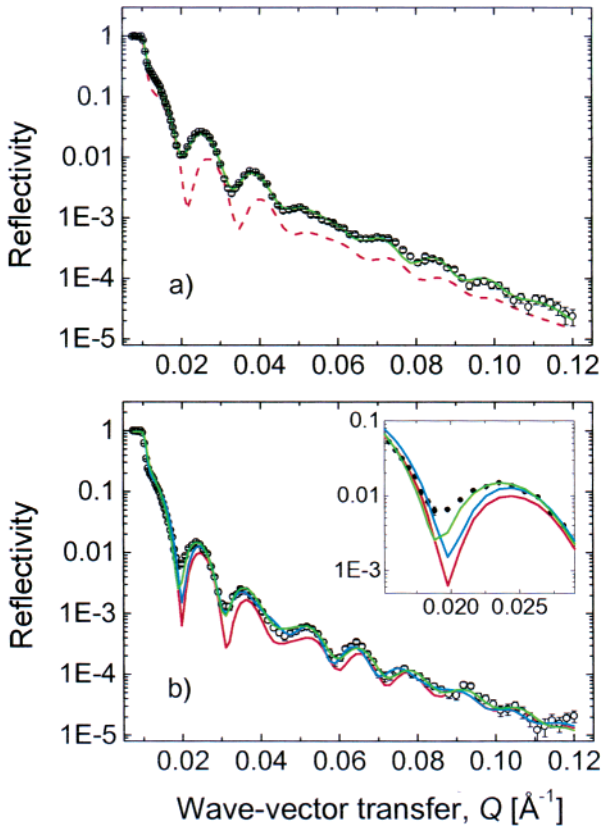

Figure 6. Comparison of the experimental data (circles) and calculated neutron reflectivity profiles for C18 (a) and sample II of C11OH (b). (a) Dashed red line: the model assuming the SAM is in direct contact with the bulk water phase (one-box model) with substrate parameters adopted from the dry-state experiment. Green line: the model assuming two IW layers of reduced density are between the SAM and the bulk water phase (three-box model). (b) Red line: the model assuming the SAM is in direct contact with the bulk water phase (one-box model). Green line: the model assuming two IW layers of reduced density are between the SAM and the bulk water phase (three-box model). Blue line: the model assuming two IW layers of increased density are between the SAM and the bulk water phase (three-box model). The differences of the profiles are magnified in the insert.

OEG SAMs.[21,37] Both the higher density and the hydrophobic nature of the poly(methylene) spacer prevent penetration of water molecules into the film. The experimental data and box-model results for C18 are displayed in Figure 6a. The corresponding fitting parameters are summarized in Table 2a, together with the $(\chi_1^2/\chi_2^2)^{1/2}$ values for the two-box model and $(\chi_1^2/\chi_3^2)^{1/2}$ for the three-box model.

Figure 6a shows that the assumption of bulk water directly contacting the hydrophobic C18 SAM is inconsistent with the experimental results. To fit the one-box model to the reflectivity data would require the assumption of a metal layer thickness of 545 Å, which is more than 30 Å higher than the value determined from the dry-state experiment and does not correspond to the estimated thickness from the width of the Kiessig fringes of 513 ± 15 Å. Therefore, we used the substrate data determined from the dry-state experiment as fixed input parameters for the one-box model and the calculation of χ_1^2.

Comparing the model calculations to the experimental data, we find that neither the one-box model with fixed substrate parameters (Figure 6a, dashed red line) nor the two box-model can satisfactorily describe the interfacial properties. It appears that the density gradients in the near-surface region are so high that the water interphase has to be split into two distinct boxes as approximated by a three-box model (Figure 6a, green line). Here, indeed, excellent agreement between the model and measured reflectivity data is obtained. The low scattering length density as observed for IW_1 might be related to the formation of nanoscopic air bubbles at hydrophobic surfaces as reported by Ishida et al.,[24] Ederth et al.,[25] and Tyrell et al.[26]

In the case of C11OH in contact with D_2O, no unique solution of the interphase composition could be found to explain the experimental data. Again, a three-box model correlates best with the experimental data for the two different samples studied. However, there are now two significantly different sets of model parameters which lead to good agreement with the measured profiles. As shown in Table 2b, both the assumptions of a reduced and an enhanced interphase density compared to bulk D_2O yield high values for $(\chi_1^2/\chi_2^2)^{1/2}$ and $(\chi_1^2/\chi_3^2)^{1/2}$. Actually, considering the absolute numbers for both samples, a three-box model with a reduced water density in the interphase region is the most favored one, although intuitively, rather a bulk-water-like interphase density would be expected due to the hydrophilic character of the SAM. Again, d_{Cr+Au} differs slightly for the different models. However, the values are consistent with the dry-state experiment and the thickness estimates of the metal layers from the width of the Kiessig fringes, respectively.

Figure 6b presents the reflectivity profile for C11OH in contact with D_2O. The one-box model (red line) yields reflectivity values that are too low to fit the experimental data. The three-box models with reduced (green line) and enhanced (blue line) density show nearly identical correlation with the reflectivity measurement. The most pronounced difference between the two three-box models is found at $0.015\ \text{Å}^{-1} \leq Q \leq 0.025\ \text{Å}^{-1}$ as shown in the insert of Figure 6b. Obviously, it is not possible to extract a unique box model describing the density profile from the measurements on C11OH in contact with D_2O.

Discussion

The analysis of the neutron reflectivity data shows that a consistent interpretation of the data sets in terms of a distinct (but unexpectedly low) water density in the near-surface interphase can be achieved for the EG3-OMe-terminated alkanethiolate SAMs. For EG3-OH, a bulklike water density of the interphase is extracted from the data sets. Before we discuss these results and also the ambiguity encountered in analyzing the data for the EG6-OH, C18, and C11OH films, we first list possible problems which could lead to wrong conclusions about the SAM/water interphase.

One uncertainty is, of course, the quality of our films. Although prepared using procedures developed by us and others to ensure complete coverage and homogeneity of the films on polycrystalline and predominantly (111)-oriented gold films, the films prepared on the large quartz crystals necessary for neutron reflectivity measurements cannot be characterized directly in our apparatus by standard surface analysis techniques such as XPS and Fourier transform infrared spectroscopy due to their size. Ellipsometry and AFM were applied to some of the samples to verify the SAM thickness and surface roughness, but questions remain about their homogeneity. This should be kept in mind when discussing the fact that for some of the films the analysis is ambiguous and different samples show different results.

The quality of the films, in particular the hydrophobic ones, will inevitably also have an effect on air inclusions

Table 2. Optimized Parameters of the Two- and Three-Box Models for C18 (a) and C11OH (b) against D_2O[a]

	(a) C18 SAM		(b) C11OH SAM			
			low density		high density	
no. of samples	1	1	2	2	2	2
no. of boxes	2	3	2	3	2	3
d_{IW1} [Å]	20	21	21.5 ± 0.5	22.5 ± 1.5	126.5 ± 4.5	100.5 ± 23.5
d_{IW2} [Å]		48		43.0 ± 5.0		44.0 ± 1.0
ρ_{IW1} [$\times 10^{-6}$ Å^{-2}]	1.47	0.57	5.03 ± 0.37	3.79 ± 0.02	6.81 ± 0.01	6.92 ± 0.90
ρ_{IW2} [$\times 10^{-6}$ Å^{-2}]		5.61		5.78 ± 0.11		6.59 ± 0.05
$\rho_{IW1}/\rho_{BW} \times 100$ [%]	23.1	9.0	78.8 ± 5.8	59.4 ± 0.3	106.6 ± 0.1	108.4 ± 1.5
$\rho_{IW2}/\rho_{BW} \times 100$ [%]		87.9		90.6 ± 1.7		103.3 ± 1.2
$(\chi^2_1/\chi^2_{2or3})^{1/2}_{1/R}$	7.55	24.89	1.24−1.96	2.09−2.51	1.47−1.87	1.23−2.44
$(\chi^2_1/\chi^2_{2or3})^{1/2}_{1/\Delta R}$	4.71	38.64	1.13−1.21	1.27−1.37	1.04−1.38	1.37−1.44

[a] The number of samples used to derive the results is given in the third line.

or the presence of "nanobubbles" as observed in AFM work. Due to the unexpectedly low water density at the EG3-OMe SAMs, we conducted a series of experiments with air-saturated and degassed deuterated water. These measurements are not conclusive yet due to the problems associated with replacing the degassed alcoholic thiol solution used for film preparation with degassed water while avoiding residual ethanol incorporation in the films. At this stage, we can report only that we do find small differences in the reflectivity curves with degassed water (as compared to air-equilibrated ambient water) for the EG3-OMe samples, but not for the hydrophilic hydroxy-terminated SAMs. This indicates that there may be problems associated with interpreting experiments on the nature of solid/water interfaces conducted under ambient conditions (but note, this is the natural environment) under the assumption that no gas inclusions are present. It should be kept in mind also in the following discussion that air inclusions or nanobubbles could cause variable results on supposedly identical samples or might be the reason for the low water density on the hydrophobic surfaces as concluded from the best fits to the reflectivity curves.

A systematic source of error or gross simplification is in the procedures used to fit the data. Problems are the use of a "box" model for the SAM and the interphase water which takes into account only in a simplified way the diffuse character of the SAM/water interface, and even more so the gradient in water density from the SAM into the bulk water. We assume Gaussian roughness. This made the Névot and Croce approach applicable to our data. Following this route, one has to keep in mind that the numbers that are extracted from the box model can be misleading unless interpreted with consideration of the substantial smearing. It is the $\rho(z)$ profile which represents the interface and not a box i of constant ρ_i which dominates the reflectivity in this case.

Despite these uncertainties in the film quality, possible gas inclusions, and the reliability of the fitting procedures, a consistent model is derived for some of the films, whereas for others different data give contradictory results or nonphysical models if the possibility of air inclusions or nanobubbles is ignored. In the following, we first discuss the data on the EG3-OMe SAMs, which have been studied most extensively to establish the reproducibility of the neutron reflectivity measurements and for which a comparison to GCMC simulations[2] can be made. For the four EG3-OMe samples studied in D_2O and the one in the QMC D_2O/H_2O mixture, the variation of the SAM thickness within plausible limits and the water content in the film result in a model with a water interphase of reduced density as compared to that of bulk water, the mean values being 41.3 (41.8) Å for thickness and 86.4 (86.9)% for density (Table 1a).

Unfortunately, a straightforward comparison of these quantities with those found in GCMC simulations[2] is impossible because the measurements and the simulations deal in essence with different systems: while the simulations are concerned with water confined between two parallel SAMs, the experiments deal with a single SAM−ambient water interface, which formally corresponds to infinite separation between the parallel SAMs. For the EG3-OMe SAMs whose substrates are a distance $H = 80$ Å apart, the average water density in a 20 Å thick layer near the SAM surface was simulated to be 92.2% of bulk water density (Figure 2), which is noticeably higher than the value derived from the parameter fitting to the neutron reflectivity curves (86.3%). With increasing H, the combined effect of the two opposite SAMs on the confined water should decay, and the interphase water density should increase, so that the agreement between the simulations and experiment can only become worse. An approximate extrapolation of the simulation results at different H to the infinite separation showed that the average density depression in the 20 and 30 Å thick interphase water layers cannot exceed 3.5 and 2.5%, respectively, which is much less than observed experimentally. The allowance for the SAM imperfectness had a similar effect: the interphase water density rose, which added to the discrepancy between the simulation and experiment.

We finally address the results obtained on the hydroxy-terminated oligo(ethylene glycol) and the C11OH SAMs. No explicit simulations or predictions are available about water density at these hydrophilic surfaces, which eliminates the possibility to make a direct comparison between the data and simulations. On the EG3-OH surfaces, our experiments, both in D_2O and BSA-MC, are best explained by assuming that the water density at the interface is very close to the bulk density. The same conclusion is reached for the EG6-OH surface studied at the D17 spectrometer in Grenoble, whereas the sample investigated at BENSC in Berlin can be fitted only by assuming a reduced density water interphase similar to the one found at the more hydrophobic EG3-OMe surface. This discrepancy and the inconclusive results for the C11OH films, which can be explained by either a reduced or bulklike density at the interface, clearly show the ambiguities involved in interpreting the data. Intuitively, we expect a bulklike water layer at these hydrophilic SAM surfaces, but this assumption needs to be tested in further experiments.

From the analysis of our NR experiments, we determine a substantial deficit of water density at the hydrophobic

C18 interface, as a matter of fact much too large to be explained by the hydrophobicity of the surface (Table 2a). We suspect that nanoscopic air inclusions in the hydrophobic film, or air nanobubbles as decribed in recent AFM experiments,[24−26] are present under our experimental conditions and lead to the anomalous results.

We conclude that NR experiments are able to distinguish between the densities of water in contact with SAM surfaces of different wettabilities but that without solving the phase problem in the scattering experiments no definite conclusions can be drawn for the present case. The "best fit" approach using a box model is not sufficient to analyze the reflectivity data in detail and to draw unambiguous conclusions based on the data with the presently accessible Q range. The Q range corresponds to distances in real space down to $\sim 2\pi/Q_{max} \cong 50$ Å, implying that differences in the density profile much below this length scale are difficult to distinguish. The situation may be complicated by variable defect densities in the organic surfaces and the presence of nanobubbles in the experiments which so far have not been considered in any simulation work. More sophisticated experimental work and simulations are required before a more definite statement can be made regarding the exact profile of the interface density of water at a solid surface.

Conclusions

For EG3-OMe-terminated undecylthiolate SAMs on Au, experimental evidence has been found for the presence of an unexpectedly extended density-reduced interphase water layer next to the SAM surface. The mean values as determined from the characterization of different samples within the presently accessible Q range were a layer thickness of about 4 nm and a density of approximately 85−90% compared to bulk water, in significant disagreement with the results of GCMC simulations for these SAMs in contact with liquid water. A similar low interphase water density was observed for one of the EG6-OH-terminated undecylthiolate SAMs on Au, whereas a second sample revealed a bulklike water density. In the case of EG3-OH, the deviation from bulk water appears to be minor. Because for EGn-terminated SAMs in contact with D_2O it is difficult to appreciate the differences between the one- and two-box models by eye, statistical methods have been used to evaluate the significance of the different models. These techniques confirm the conclusions drawn.

For comparison, we also studied the interfacial water density for hydrophobic octadecanethiol (C18) and hydrophilic 11-mercapto-1-undecanol (C11OH) SAMs on Au. In the case of C18, a second interfacial layer is required to achieve a satisfactory agreement between the experimental data and the model calculations. For C18, the measured reflectivity profiles suggest an interfacial water structure comprising a ∼2 nm thick layer with only ∼ 9% bulk D_2O density, followed by a ∼5 nm thick layer with ∼88% bulk D_2O density. These results are suspected to be obscured by the presence of air nanobubbles at the hydrophobic interface.

In the case of C11OH, no unique model representing the measured data could be identified. Both the assumptions of a density-reduced and a density-enhanced interfacial water structure yielded good agreement with the experiment.

The question of to what extent microscopic air bubble formation at the water/SAM interface may contribute to the measured water density distributions is still being investigated.

Acknowledgment. We thank the Bundesministerium für Bildung und Forschung, the Office of Naval Research, the Deutsche Forschungsgemeinschaft, and the Fond der Chemischen Industrie for financial support. We also thank Robert Cubitt from ILL/Grenoble for his assistance at D17 and Jürgen Pipper for his help during the first experiments at V6. F.S. acknowledges useful discussions with R. K. Thomas.

Supporting Information Available: Detailed fitting results, including substrate parameters and SAM roughness. This material is available free of charge via the Internet at http://pubs.acs.org.

LA026716K